

# THE INTERANNUAL OSCILLATION OF RAINFALL OVER CHINA AND ITS RELATION TO THE INTERANNUAL OSCILLATION OF THE AIR-SEA SYSTEM\*

*Chen Longxun* (陈隆勋),

Academy of Meteorological Science, SMA, Beijing

*Chen Duo* (陈多),

Guangzhou Central Meteorological Observatory, Guangzhou

*Shen Rugui* (沈如桂)

The Atmospheric Science Department, Zhongshan University, Guangzhou

and *Zhang Qingfen* (张清芬)

Academy of Meteorological Science, SMA, Beijing

Received December 9, 1989

## ABSTRACT

The quasi-biennial oscillation (QBO) and 3.5 years quasi-periodic oscillation (named TO hereafter) are exhibited in most of 48 weather stations of China by applying power spectrum analysis to the monthly rainfall data for the period from Jan. 1933 to Dec. 1987.

In order to reveal the features of QBO and TO components, another rainfall data set in 160 stations over China for the period from Jan. 1951 to Dec. 1987 was analysed by means of a new method named complex empirical orthogonal function (CEOF). The results show that both QBO and TO modes exhibit two propagation ways: one originates in Northeast China, extends southward, passes through North China and reaches the eastern part of Northwest China and the northern part of Southwest China; the other appears over Guangdong and Fujian, then moves northward and westward respectively to the Huanghe-Huaihe Basin and Southwest China. These two paths of oscillation meet over North China and the area between the Changjiang River and the Huanghe River.

A significant correlation exists between the interannual oscillation of the rainfall over China and that of the sea surface temperature (SST) at the equator. Although the correlation between the rainfall over China and the SST over the equatorial eastern Pacific is rather weak, the correlation between their oscillation component is pronounced.

## 1. INTRODUCTION

The QBO was first found by Reed et al. (1961) in the equatorial lower stratospheric zonal winds. Since then, many authors have examined whether the QBO is evident in the troposphere

---

\* This work is supported by the National Natural Science Foundation of China under program 4860210 and the Foundation of Tropical Meteorology, SMA.

and outside the equator, and they have found that it is but with a different strength. For instance, Rasmusson et al. (1981) found the QBO signal in the time series of surface temperature over the United States, Trenberth et al. (1984) indicated significant QBO evidence in sea level pressure over the Northern Hemisphere. Yasunari (1985) noted that the QBO signal exists in zonal wind in the troposphere over the equator and is closely related to the El Niño event. Yan et al. (1988) and Chen et al. (1989) also showed the existence of QBO in SST, which is coupled with QBO of sea level pressure and zonal wind.

Also a number of researchers found the 3.5-year quasi-periodic oscillation (called TO hereafter) in many tropical meteorological parameters, such as the Southern Oscillation index, the rainfall over India (Bhalme and Jadhav, 1984) and the zonal wind in troposphere (Yasunari, 1985). Yasunari (1987) and Krishnamurti et al. (1988) revealed the evolution of the TO in zonal wind and in sea level pressure. Yan et al. (1988) and Chen et al. (1989) indicated the evidence of TO in SST and discussed the TO variation of SST by using an extended EOF method. It is found that TO of SST is coupled with that of sea level pressure quite well.

As described above, QBO and TO seem to be widespread in meteorological parameters throughout the atmosphere. Thus, some considerations come up to us. Firstly, what is the evidence of QBO and TO in the area of China and how do they develop? Secondly, the climate variation over China on ten-year scale is related to the interaction of air-sea-earth system, then do the interannual oscillations QBO and TO in air-sea system affect the climate of China and how do they work? Finally, as far as the El Niño event is concerned, since SST in the equatorial eastern Pacific (EPPSST) has much less correlation with the rainfall over China than over India, is it possible that the correlation between the oscillations of SST and those of rainfall over China would become more significant? If so, how do they interact with each other? Those are just what this paper aims at. Analysed objects are rainfall and surface air temperature over China. This paper presents the results about rainfall only, and those about temperature are given in another paper. As for the rainfall over China, Huang (1988) analysed QBO and pointed out that QBO appeared clearly over North China, and over the middle and lower reaches of the Changjiang River, and was a propagating wave from east to west.

## II. DATA AND METHOD OF ANALYSIS

The data used here is the monthly rainfall from Jan. 1951 to Dec. 1987 over 160 selected stations in China. But in the power spectrum analysis, only 48 stations are selected with the data extending till Jan. 1933. There are some data missing in some years, especially in 1948—1949 for some reasons. Therefore, we use a linear interpolation to complete the whole time series. The interpolation value is reasonable because it does not show any unfitness for the power spectrum analysis. The value of EPPSST used here is the average over the domain from 160°W to 100°W and from 5°S to 5°N.

The climatic monthly mean was subtracted out for each month to get an anomaly series at each station, then a power spectrum analysis method was applied to this series, so that the evidence of QBO and TO in rainfall over China can be presented. A bandpass filter (Murakami, 1979) was also used to pick up QBO and TO modes with main periods of 24-months and 40-months, respectively. Thus the filtered rainfall anomaly at time  $n$  is given by

$$\bar{R}_n = a_0(R'_n - R'_{n-2}) - b_1\bar{R}_{n-1} - b_2\bar{R}_{n-2}, \quad (n=1, 2, \dots, N)$$

where

$$a_0 = \frac{2\Delta\Omega}{4 + 2\Delta\Omega + \Omega_0^2}, \quad b_1 = \frac{2(\Omega_0^2 - 4)}{4 + 2\Delta\Omega + \Omega_0^2}, \quad b_2 = \frac{4 - 2\Delta\Omega + \Omega_0^2}{4 + 2\Delta\Omega + \Omega_0^2},$$

$$\Delta\Omega = 2 \left| \frac{\sin(\omega_1 \Delta t)}{1 + \cos(\omega_1 \Delta t)} - \frac{\sin(\omega_2 \Delta t)}{1 + \cos(\omega_2 \Delta t)} \right|, \quad \Omega_0^2 = \frac{4 \sin(\omega_1 \Delta t) \sin(\omega_2 \Delta t)}{(1 + \cos \omega_1 \Delta t)(1 + \cos \omega_2 \Delta t)}$$

where  $R'_n$  is the value at time  $n$  before filtering, and  $N=444$  is the length of data. We also set  $\Delta t=1$ ,  $\Delta T=7$ , and the main period  $T$  equal to 24 (months) and 40 (months), and then  $\omega_0=2\pi/T$ ,  $\omega_1=2\pi/(T-\Delta T)$ ,  $\omega_2=\omega_0^2/\omega_1$ , with respect to different values of  $T$ .

To investigate QBO and TO modes of rainfall, a new analysis of CEOF is used. For the filtered anomaly series  $R_j(t)$ , where the subscript  $j$  is a spatial position index and  $t$  is time, by using the Hilbert transform, we have

$$\hat{R}_j(t) = \sum_{-\infty}^{\infty} R_j(t-i) h(i),$$

where

$$h(i) = \begin{cases} \frac{2}{\pi i} \sin^2\left(\frac{\pi i}{2}\right), & i \neq 0 \\ 0, & i = 0 \end{cases}$$

Then a new complex time series  $R_j(t) = R_j(t) + i\hat{R}_j(t)$  is formed, where  $R_j(t)$  is the real part of  $R_j(t)$  and  $\hat{R}_j(t)$  is the imaginary part. It is the  $R_j(t)$  that can reveal the features of the original time series at different times. Theoretically,  $i=\infty$  in (1), but the sum must be truncated in practice, and  $i$  is taken the value of 7—25 which is suitable for the calculation. We set  $i=12$  here.

The covariance matrix of  $U(u=v_{jk})$  is given by

$$U_{jk} = \frac{1}{T} \int_{-T/2}^{T/2} \hat{R}_j(t) \hat{R}_k^*(t) dt,$$

where  $T$  is the time domain defined by the time series.  $\hat{R}_k^*(t)$  is the complex conjugation and  $U$  is a Hermite matrix.

The expansion of  $\hat{R}_j(t)$  is expressed as

$$\hat{R}_j(t) = \sum_n A_n(t) B_n(j),$$

where the complex time-dependent principal component is given by

$$A_n = \sum_j \hat{R}_j(t) B_n(j),$$

with proper normalization  $\langle B_n B_n^* \rangle = \delta_{nm}$  and hence  $\langle A_n A_m^* \rangle = \delta_{nm} \lambda_n$ , where  $\lambda_n$  and  $B_n(j)$  are the real eigenvalue and complex eigenvector corresponding to Hermite matrix  $U$ , respectively.  $\delta_{nm}=1$  for  $n=m$ , otherwise,  $\delta_{nm}=0$ , and  $\langle \quad \rangle$  denotes the average of the series.

Thus, the contribution of the  $k$ th complex principal component to the total variance is

given by  $\lambda k / \sum_{m=1} \lambda_m$ . The  $k$ th ( $k=1, 2, \dots, n$ ) eigenpattern has four measures of spatial phase

function  $\theta_k(t)$  and temporal amplitude function  $A^k(t)$ . If conjugation is denoted by asterisk, and imaginary and real parts by Im and Re, these four measures are given by

$$\theta_k(j) = \arctan[\text{Im} B_k(j) / \text{Re} B_k(j)], \quad A^k(j) = [B_k(j) B_k^*(j)]^{1/2}, \\ \theta_k(t) = \arctan[\text{Im} A_k(t) / \text{Re} A_k(t)], \quad A^k(t) = [A_k(t) A_k^*(t)]^{1/2}.$$

Finally, we also reconstructed a field corresponding to the former eigenvector and composed a field of 8 phases in accordance with the temporal phase  $0, \pi/4, \pi/2, 3\pi/4, \pi, 5\pi/4, 3\pi/2,$  and  $7\pi/4,$  respectively.

III. THE FEATURES OF INTERANNUAL OSCILLATION OF RAINFALL OVER CHINA

A power spectrum analysis was applied to rainfall anomalies of 48 weather stations over China, respectively. The curves of power spectra at some stations are displayed in Fig.1. The figure shows that the period with a power spectrum peak value and significant level higher than 0.05 is about 2 years at some stations or 3.5 years at others.

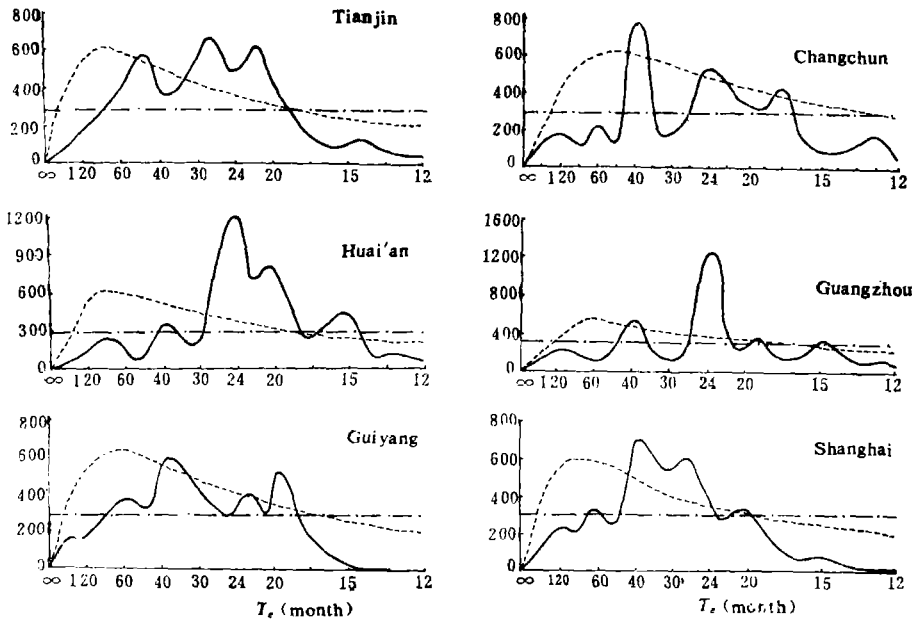


Fig. 1. The power spectra of monthly rainfall series at Tianjin, Huai'an, Guiyang, Changchun, Guangzhou, and Shanghai, respectively. Heavy lines represent the power spectra, dashed lines and dot-dashed lines denote respectively the red-noise with 0.05 significant level and the check of no-main-period.

Two figures (omitted) are drawn to present the distribution of power spectra of QBO and TO, respectively. For QBO, the power spectrum value at all but three stations has passed the red-noise test. The periods with peak value are within 18—29 months. The mean over 46 stations is 23.39 months and set to be 24 months. The distribution of power spectra also shows that areas with high value of QBO power spectrum are located over Northeast China, North China, the eastern part of Northwest China, the middle and lower reaches of the Changjiang River, the east of Qinghai-Xizang Plateau and Guangdong-Hunan region. Regions with low value are over Inner Mongolia, Xinjiang. Qinghai, Guangxi, Guizhou and the reaches of the Huaihe River. Our results show great similarity to those presented by Huang (1988) and even more details.

For 3.5 year oscillation, it is indicated that 17 of 48 stations fail to pass the red-noise test. in other words, only 65 percent of the stations pass the test with an average of 38.87 months. We assume the period of the 3.5 year oscillation of rainfall to be 40 months. We also find that

the 3.5 year oscillation of rainfall is active in regions such as the western part of North China, the eastern part of Northwest China, the northern part of Northeast China, and Guangdong. On the other hand, it is insignificant over the middle and lower reaches of the Changjiang River, Sichuan and Yunnan. Consequently, both TO and QBO are significant over Northeast China, Guangdong and the western part of North China, and insignificant over Guangxi and Guizhou. Over other regions, only one kind of oscillation is significant, for instance, over the middle and lower reaches of the Changjiang River, the QBO mode is significant but TO mode is not.

#### IV. THE CEOF ANALYSIS OF INTERANNUAL OSCILLATION

Fig.2 shows the distribution of 160 stations used in our paper. We divide these stations into 15 regions. Based on the results mentioned above, the CEOF analysis is applied to QBO and TO modes to investigate the features of their evolution in time and in space. The total variance and the percentage variance accounted for by the first six eigenvectors were shown in Table 1.

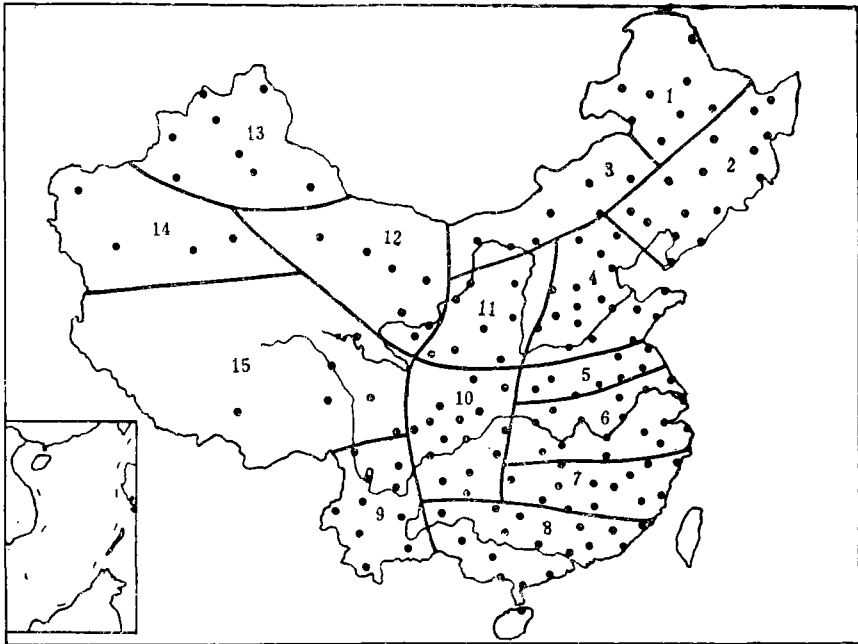


Fig. 2. The distributions of 160 weather stations in China and of 15 rainfall divisions of China.

The cumulative percentages of the first four eigenvectors for the QBO mode is 52.6% and that for the TO mode is 80.6%. The explained percentages of the first eigenvector for QBO and TO modes are 18.0% and 28.5%, respectively. Huang (1988) also did the similar research but over 35 stations, and his results showed that the first eigenvector explained percentage is 24%, higher than ours (18.0%). The causes for discrepancy may be that the data period in our analysis is seven years longer than his and the number of stations is increased by about four times. Nevertheless, the first eigenvector explained percentage of the TO mode is still very high. For both QBO and TO, the first eigenvector plays a predominant role in all eigenvectors. Therefore, the amplitude function and the phase function of the first eigenvector can be used to express the main spatial-temporal features of these oscillation. We will mainly discuss

the first eigenvector in the following.

Table 1. The First Six Eigenvector Percentages Explained and Cumulative Percentages Explained by the CEOF Analysis of Rainfall's Interannual Oscillation

Mode	Eigenvector	1	2	3	4	5	6
QBO	Percentages explained	18.0	14.8	10.7	9.1	7.6	6.7
	Cumulative percentages explained	18.0	32.8	43.5	52.6	60.2	66.7
TO	Percentages explained	28.5	22.8	18.7	10.6	6.2	5.2
	Cumulative percentages explained	28.5	51.3	70.0	80.6	86.8	92.0

The spatial amplitude distributions of the first eigenvector for QBO and TO modes are shown in Figs. 3a and 3b. For the QBO mode, there are some high value regions over North China, the middle and lower reaches of the Changjiang River, which show quite consistence with Huang's results. For the TO mode, the high value areas lie over Northeast China, Hebei, Gansu, Qinghai, the Huanghe-Huaihe Basin, Guangdong and Fujian. Besides, a less high value region lies over the middle and lower reaches of the Changjiang River. We also find that over some places such as Shanxi and Shaanxi, the amplitude is rather large for QBO but very small for TO, while over other places such as Gansu, Qinghai, and the northern Sichuan, the amplitude is small for the QBO mode but large for the TO mode. Thus the QBO mode is opposite to the TO mode in strength except over the eastern part of North China and the middle and lower reaches of the Changjiang River, where both oscillations are strong. For this reason, the geographic location should be considered while discussing the interaction between oscillations.

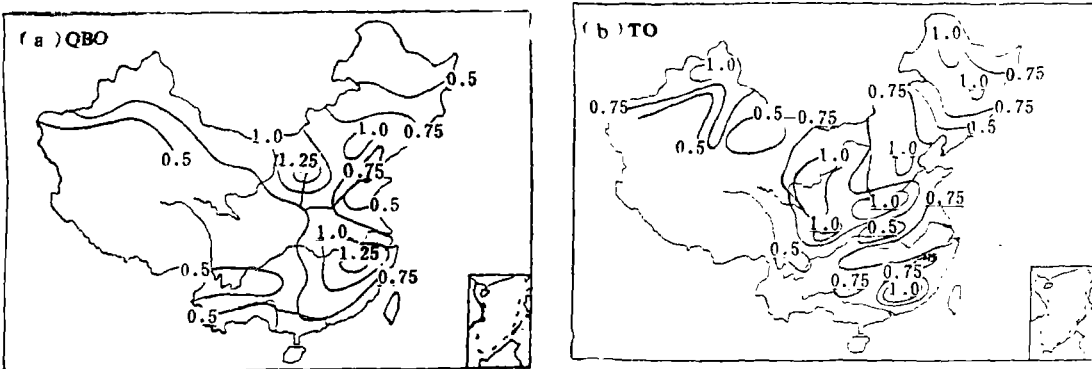


Fig. 3. The spatial amplitude distribution for the first eigenvector of interannual oscillation of China's rainfall. (a) QBO mode, (b) TO mode.

The spatial phase function distributions of the first eigenvector for QBO and TO modes are also made (figures omitted). The results indicated that the propagating features of QBO mode are consistent with those of TO mode. In zonal direction, they both propagate westward; in meridional direction, there are two propagation ways: one is from the north to the south, and the other is from the south to the north. These two ways meet over North China for QBO mode and over the region between the Huanghe River and the Huaihe River for TO mode about

35°N. Thus for both QBO and TO, there are two oscillation sources for propagation. One is in the South China Sea and the Western Pacific, which affects the climate of China by moving in SSE-NNW direction through Guangdong and Fujian to North China and Southwest China. The other is propagating in NNE-SSE direction through Northwest China to North China and the eastern part of Northwest China. Thus, over 35.0°N–40.0°N these two modes meet. It is also indicated that north-south propagating is dominant over the eastern China and the east-west propagating over the western China. However, some differences still exist. The main one is that the QBO mode has much more south-north moving component, but the TO mode has much more east-west moving component. And this is also different from Huang's results, which did not mention the northward propagation of the QBO mode.

The temporal amplitude and temporal phase of the first eigenvector for QBO and TO are also analysed (figures not shown). The temporal amplitude function of the QBO mode shows peak values in years 1954, 1964, 1967–1968, 1973, and 1982–1983, while that of the TO mode in years 1954–1955, 1965–1966, 1968, 1972–1973, and 1980. Comparing these years with the years El Nino event occurred (in 1953, 1957, 1963, 1965, 1969, 1972, 1975–1976, 1979, and 1982–1983) we can see that in the El Nino year or its following year, the temporal amplitude of rainfall has a peak value, especially in these strong El Nino signal years, such as 1982–1983.

Using the temporal phase function, we can set the months which have an identical phase and then reconstruct the corresponding field of the first eigenvector and compose them at different temporal phases.

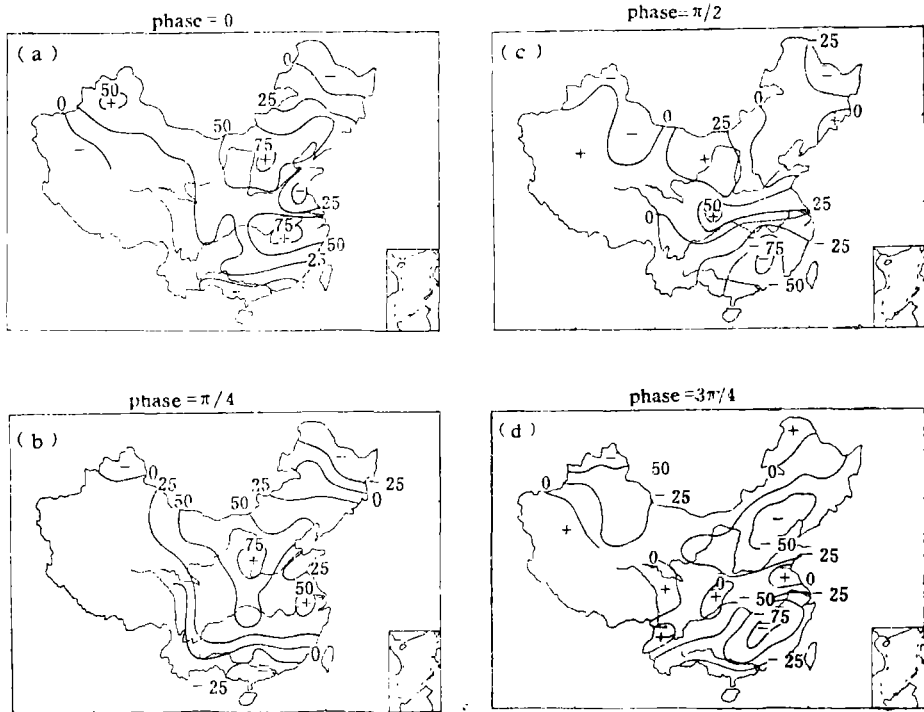


Fig. 4. The phase composite field reconstructed from the corresponding fields of the first eigenvector of QBO mode of rainfall. (a) phase 0(month 0), (b) phase  $\pi/4$  (month 3), (c) phase  $2\pi/4$  (month 6), (d) phase  $3\pi/4$  (month 9).

Figs. 4a—d give the composition of the reconstructed corresponding fields of the first eigenvector for QBO. The phases 0,  $\pi/4$ ,  $2\pi/4$ , and  $3\pi/4$  correspond to months 0, 3, 6, and 9, respectively. The field of the phase 0— $3\pi/4$  is identical with that of  $\pi-7\pi/4$  but with opposite sign. In Fig. 4 we note that at month 0 (phase 0, Fig. 4a), it is negative over Northeast China, South China, the region between the Changjiang River and the Huaihe River, but positive over North China, Xinjiang, and the middle and the lower reaches of the Changjiang River. Three months later, i.e. when phase= $\pi/4$  (Fig. 4b), the negative area over Northeast China and the positive area over North China extend west-southwestward. Another negative area over South China extends northward, but the positive area over the middle and lower reaches of the Changjiang River weakens. Another three months later, i.e. when phase= $2\pi/4$  (Fig. 4c), the negative area over Northeast China has extended to North China and the original positive value over North China extended south-southwestward to the eastern Sichuan. The negative area over South China moves northward to the middle and lower reaches of the Changjiang River about  $30^\circ\text{N}$  and forms a new negative center near Jiangxi. By the time of month 9, i.e. when phase= $3\pi/4$  (Fig. 4d), two negative value centers appear over North China and south of the Changjiang River, respectively, while two positive centers are located over the Huaihe basin and Sichuan, respectively. That is, the rainfall over China is influenced by propagating oscillation from two directions. One comes from the north through Northeast China, then moves south-southwestward to the upper reaches of the Changjiang River such as Sichuan. The other one comes from the south, first appears in South China, then moves northward to the middle and lower reaches of the Changjiang River and then the region between Huanghe and Huaihe Rivers. Meanwhile, the latter also shows some westward propagating tendency to influence the rainfall over the southern part of Southwest China.

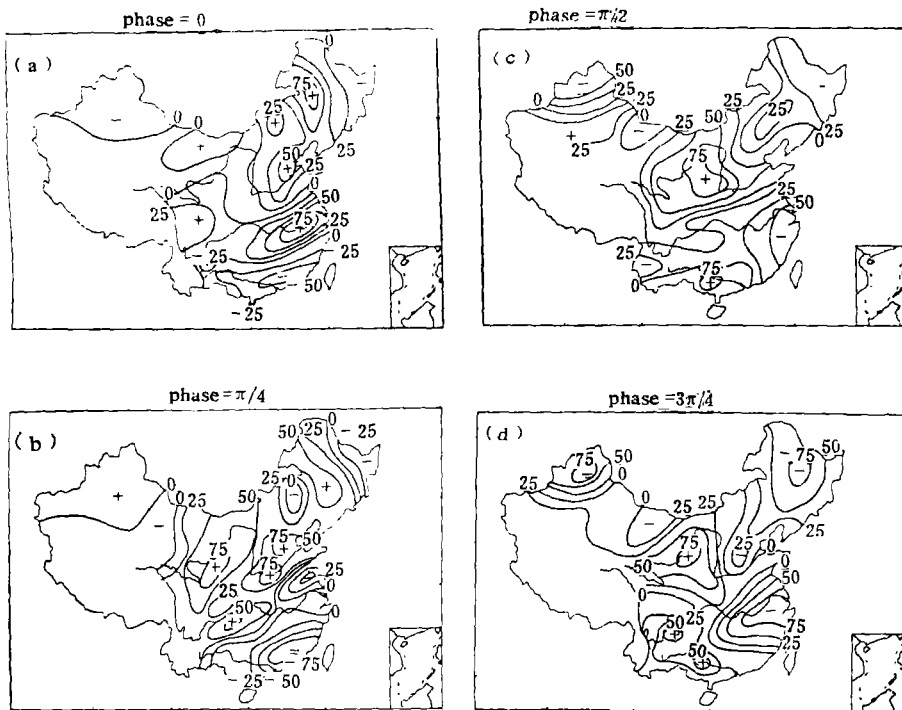


Fig. 5. As in Fig. 4 but for TO mode.

Fig. 5 is the same as Fig. 4 but for the TO mode. The temporal phases 0,  $\pi/4$ ,  $2\pi/4$ , and  $3\pi/4$  correspond to months 0, 5, 10, and 15, respectively. In Fig. 5, at phase 0 (i.e. month 0), positive regions appear over North China and the middle and lower reaches of the Changjiang River, while negative regions occur over South China and the northeastern part of Northeast China. There is also a long narrow region with minor, negative values over the Huaihe Basin. All these features are similar to those of QBO mode except for the following: (1) the positive center of TO mode over North China is close to the coast, but that of QBO mode is in Shanxi, an inland place; (2) it is positive for TO mode with a center but negative for QBO mode over the western part of Northeast China; (3) it is greatly negative for QBO mode over the region between Huanghe and Huaihe Rivers, but for TO mode, the negative areas are confined to a narrow stripe region with less intensity.

At month 5 with phase  $\pi/4$ , a negative center appears over the northern part of North China and the regional positive center over North China shifts west-southwestward. The weak negative region over the area between Huanghe and Huaihe Rivers weakens further, and the negative region over South China gets intensified and extends northward.

10 months later with a phase of  $2\pi/4$ , the negative region over Northeast China has moved to North China and the original positive center over North China has reached Shaanxi, Gansu and the northern Sichuan. In the south, the original negative center over South China shifts to the lower reaches of the Changjiang River.

To month 15 (phase  $3\pi/4$ ), negative value appear over the whole Northeast China, North China and the middle and lower reaches of the Changjiang River, while positive values are over the western China between  $100^{\circ}\text{E}$  and  $110^{\circ}\text{E}$ , northern Shaanxi and the connecting area of Sichuan and Yunnan.

As far as the TO mode is concerned, the oscillation of China's rainfall comes mainly from the source outside China. Like QBO mode, TO mode also has two ways of propagating. One comes from the north and extends in southwest direction and the other comes from the south and moves in the north-northwest direction. In other words, the former spreads from Northeast China to North China and Northwest China, while the latter moves from South China to the middle and lower reaches of the Changjiang River and to Southwest China.

Summarizing the above analyses of CEOF, we notice that the features of the QBO mode are similar to those of the TO mode, especially in the aspect of propagating. Both oscillations have sources in the north and the south, respectively, and both have a propagation component from east to west. Therefore, the influence on the interannual variation of China's rainfall may come from tropical systems at tropics as well as polar system at high latitudes. The "key region" seems to be over Northeast China, Guangdong and Fujian. And it is suggested that the sources of oscillation might be over the Sea of Okhotsk and the region from the South China Sea to the western Pacific. Over Xinjiang both QBO and TO modes are from the north and confined to this area. It is hard to find oscillations from the west, such as the Qinghai-Xizang Plateau and India, propagating into Southwest China, where oscillations are from east.

#### V. RELATIONSHIP BETWEEN THE INTERANNUL OSCILLATION OF RAINFALL OVER CHINA AND THAT OF SST

As we know, the Southern Oscillation index is correlative significantly with the air pressure and rainfall over India, but not with the rainfall and pressure over China. Although it was said that the rainfall over the reaches of the Changjiang River would increase in the year after an El Nino event happens, there are still a lot of exceptional cases. The reason, we think,

may be that the interannual variation of atmosphere is a composite of manifold interannual oscillations. Significant correlations may exist in a certain kind of oscillation, but not in composite.

For instance, using EEPSST (Jan. 1951—Dec. 1987) and the rainfall over China, we investigate the correlation between these two elements. The results indicate that (figure not shown) the maximum correlation coefficient is only 0.10. On the contrary, the correlation is quite significant for QBO and TO modes of those two elements.

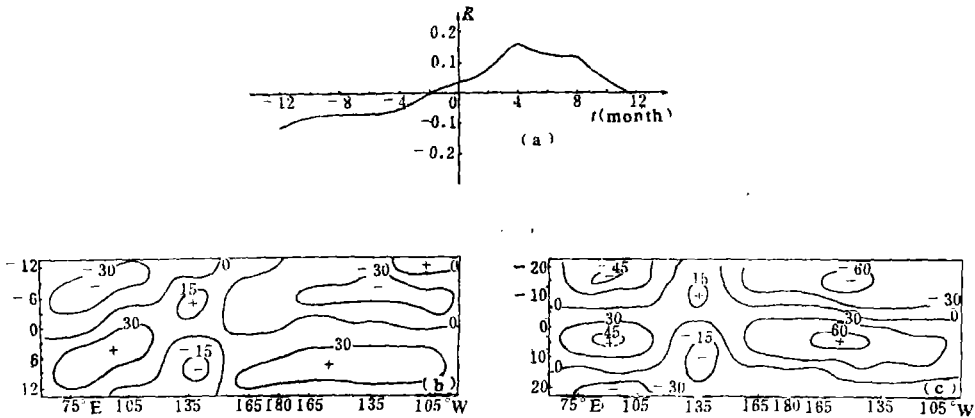


Fig. 6. The time lagged correlation between the rainfall over the middle and lower reaches of the Changjiang River and EEPSST. (a) observation amount; (b) QBO mode; (c) TO mode.

The correlation coefficients with different phase lags between SST and the rainfall over the middle and lower reaches of the Changjiang River are displayed in Fig. 6. Fig. 6a gives the correlation between the anomalies of EEPSST and rainfall and Figs. 6b and 6c demonstrate the distribution of correlation between the components of QBO and TO, respectively. We notice that, in Fig. 6a, the correlation between anomalies is insignificant. The value at month 0 is close to zero and the maximum is 0.15 when SST is 4 months ahead of rainfall. However, as shown in Figs. 6b and 6c, the correlation is rather great for both components of QBO and TO. The patterns of correlation distribution are quite similar to each other. For example, when rainfall is ahead of SST, it has a negative correlation with the EEPSST and the SST of equatorial Indian Ocean (EISST), but a positive correlation with the SST of the equatorial western Pacific (EWPSST). Yan et al. (1988) and Chen et al. (1989) pointed out that QBO and TO modes of EEPSST are in phase with those of EISST, but out of phase with those of EWPSST. Figs. 6b and 6c confirm these views again. We also notice that for both QBO and TO modes, when SST is ahead of rainfall, the correlation is positive between rainfall and EEPSST, as well as between rainfall and EISST, but negative between rainfall and EWPSST. However, the month with the maximum coefficient of QBO mode is different from that of TO mode. For QBO mode, the correlation between rainfall and EEPSST as well as between the rainfall and EISST, has a negative maximum of  $-0.30$  (which passes reliability examination) for  $-6$ -month phase-lag. For 0-month phase-lag, the correlation between rainfall and SST in the South China Sea is 0.3, and no significant correlation is found in other region. For 6-month phase-lag, it is similar to that of  $-6$  month phase-lag but with opposite sign.

**Table 2.** The Averaged Time-Lagged Correlation between the Observational Anomalies of the Rainfall over Each of 15 Divisions of China and EEPSST.

$R \backslash L$	-12	-10	-8	-6	-4	-2	0
1	-0.029	-0.012	0.029	-0.015	0.037	0.020	0.000
2	0.016	0.005	-0.015	-0.050	-0.029	-0.014	0.009
3	-0.002	-0.034	-0.019	-0.084	-0.085	-0.045	-0.072
4	0.017	-0.008	-0.015	-0.051	-0.081	-0.034	-0.038
5	-0.006	-0.010	0.004	0.038	0.013	0.009	0.010
6	-0.112	-0.079	-0.078	-0.079	-0.041	0.007	0.033
7	-0.058	-0.045	-0.044	-0.087	-0.040	0.005	0.074
8	-0.024	-0.008	-0.009	-0.050	-0.009	0.035	0.069
9	-0.005	-0.021	-0.051	-0.013	-0.034	-0.029	-0.027
10	-0.014	0.002	-0.033	-0.017	-0.061	-0.020	-0.013
11	0.018	0.007	-0.003	-0.090	-0.108	-0.090	-0.070
12	0.023	-0.028	-0.014	0.030	-0.052	-0.057	-0.046
13	-0.022	-0.059	-0.023	-0.028	-0.006	0.020	0.070
14	0.017	0.031	0.032	0.023	-0.003	-0.001	-0.003
15	0.004	0.018	-0.012	0.005	0.000	-0.013	-0.001

$R \backslash L$	+2	+4	+6	+8	+10	+12
1	0.037	0.058	0.027	0.042	0.008	0.028
2	0.017	0.007	-0.023	-0.014	-0.020	0.015
3	0.011	0.029	0.045	0.070	0.052	0.069
4	-0.032	-0.013	0.019	0.031	0.028	0.037
5	-0.011	0.022	-0.015	-0.026	-0.050	-0.074
6	0.078	0.156	0.133	0.126	0.044	-0.008
7	0.051	0.092	0.070	0.052	0.028	0.025
8	0.027	0.023	0.017	0.011	-0.003	0.008
9	-0.002	-0.010	0.016	0.019	0.030	0.050
10	-0.002	0.022	0.035	0.029	0.019	0.010
11	-0.045	0.043	0.049	0.081	0.060	0.054
12	-0.014	0.031	0.033	0.083	0.052	0.019
13	0.092	0.131	0.106	0.094	0.077	0.046
14	-0.006	-0.006	-0.008	-0.012	0.004	0.002
15	-0.005	-0.032	-0.045	-0.044	-0.014	-0.010

$R$  means "region" and  $L$  lag month.

Table 3. Same as Table 2 but for QBO Mode

<i>R</i> \ <i>L</i>	-12	-9	-6	-3	0	+3	+6	+9	+12
1	-0.185	-0.071	0.084	0.145	0.147	0.085	-0.009	-0.932	-0.094
2	-0.031	-0.183	-0.212	-0.096	0.045	0.136	0.128	0.048	-0.041
3	0.025	-0.127	-0.225	-0.214	-0.099	0.046	0.146	0.159	0.100
4	0.142	-0.030	-0.204	-0.263	-0.167	0.017	0.168	0.210	0.137
5	-0.030	+0.004	0.049	0.091	0.106	0.071	-0.007	-0.093	-0.142
6	-0.094	-0.286	-0.339	-0.191	0.094	0.352	0.426	0.271	-0.016
7	-0.176	-0.392	-0.405	-0.186	0.148	0.402	0.435	0.251	-0.040
8	-0.209	-0.255	-0.150	0.037	0.189	0.210	0.100	-0.053	-0.147
9	+0.010	-0.094	-0.143	-0.130	-0.079	-0.010	0.066	0.119	0.125
10	-0.026	-0.074	-0.098	-0.076	-0.011	0.054	0.078	0.053	0.007
11	0.198	-0.060	-0.334	-0.443	-0.309	-0.010	0.273	0.396	0.317
12	0.137	0.030	-0.120	-0.214	-0.183	-0.053	0.095	0.179	0.173
13	-0.151	-0.233	-0.200	-0.051	0.120	0.241	0.242	0.123	-0.049
14	0.173	0.129	0.036	-0.069	-0.143	-0.160	0.097	0.019	0.129
15	-0.028	-0.004	0.011	0.019	0.023	0.016	0.006	0.008	0.013

Table 4. Same as Table 2 but for TO Mode

<i>R</i> \ <i>L</i>	-20	-15	-10	-5	0	+5	+10	+15	+20
1	-0.187	-0.344	-0.300	-0.098	0.122	0.261	0.239	0.093	-0.080
2	-0.030	0.007	0.047	0.043	-0.009	-0.061	-0.088	-0.062	0.010
3	0.216	0.026	-0.210	-0.321	-0.226	0.021	0.260	0.330	0.193
4	0.148	0.015	-0.141	-0.228	-0.181	-0.011	0.152	0.205	0.130
5	-0.148	0.040	+0.205	0.232	+0.103	-0.105	-0.256	-0.236	-0.059
6	-0.542	-0.698	-0.455	0.056	0.541	0.711	0.470	-0.034	-0.502
7	-0.262	-0.094	0.097	0.244	0.293	0.215	0.004	-0.227	-0.342
8	0.074	0.225	0.237	0.133	-0.014	-0.131	-0.172	-0.127	-0.029
9	0.052	-0.089	-0.199	-0.196	-0.065	0.108	0.234	0.224	0.081
10	0.202	-0.044	-0.276	-0.342	-0.195	0.075	0.307	0.354	0.187
11	0.574	0.275	-0.190	-0.522	-0.490	-0.144	0.267	0.467	0.359
12	0.283	0.071	0.168	-0.275	-0.190	0.013	0.183	0.200	0.070
13	-0.278	-0.404	-0.304	-0.033	0.258	0.392	0.289	0.025	-0.229
14	0.288	0.261	+0.086	-0.128	-0.251	-0.244	-0.068	0.125	0.241
15	0.064	0.082	0.037	-0.051	-0.123	-0.104	-0.025	0.074	0.137

Now, we discuss the time-lagged correlation between EEPSSST and the rainfall over different parts of China. Table 2 gives the correlation between observational anomalies of EEPSSST and those of rainfall over China. Tables 3 and 4 are the same as Table 2 but for QBO and TO modes, respectively. The 15 divisions in China are displayed in Fig. 2. In the tables, negative month denotes the rainfall is ahead of the SST, i.e. “-” month means the influence of rainfall on SST, and vice versa. We can see in Table 2 that for the observational amount, there is no significant correlation. But for the QBO mode (Table 3), the areas with maximum value and “+” month are Regions 6 (the middle and lower reaches of the Changjiang River), 7 (Fujian, Jiangxi and Hunan), and 11 (Shaanxi, Gansu and Ningxia). The values are between 0.369—

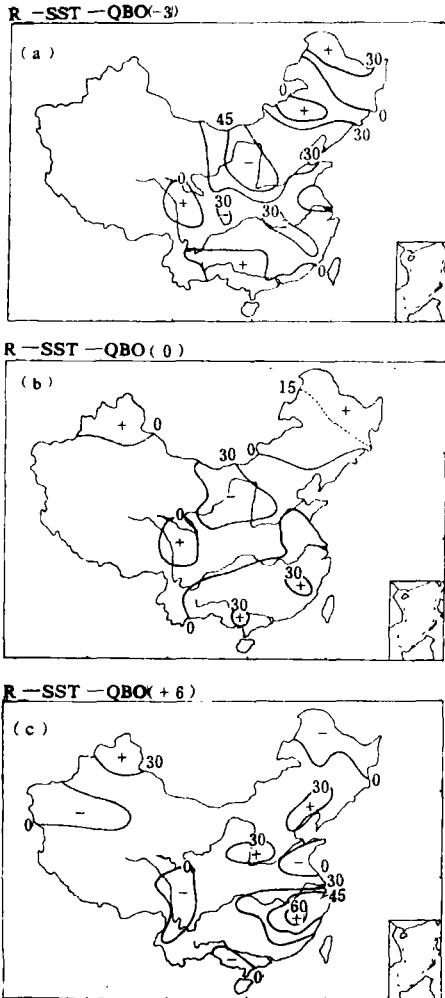


Fig. 7. The distribution of time-lagged correlation between QBO mode of China's rainfall and EEPSSST at different time-lagged phases. (a) -3 month; (b) 0 month; (c) +6 month.

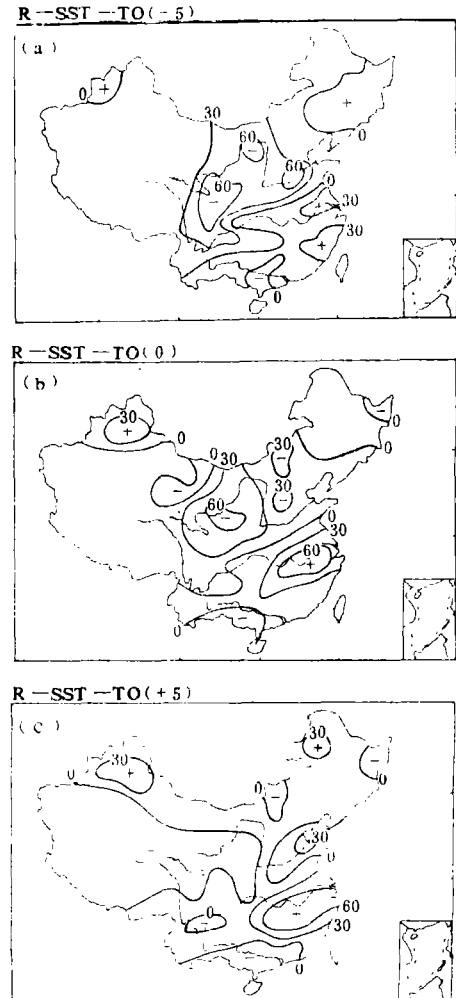


Fig. 8. As in Fig. 7 but between TO modes. (a) -5 month; (b) 0 month; (c) +5 month.

0.435, and the lag month is +6 months in Regions 6 and 7, +9 months in Region 11 implying a center moving from south to north. For the TO mode (Table 4), these areas are Regions 6, 10 (Shaanxi, Sichuan), 11 and 13 (northern Xinjiang). The maximum values range from 0.289 to 0.711 with lag month from +10 to +20. Therefore, it is seen that for both QBO and TO modes, the middle and lower reaches of the Changjiang River, Shaanxi, Gansu and Ningxia are regions with maximum correlation. But, the lag-month with maximum for the QBO mode is different from that of TO mode. Figs. 7 and 8 provide the correlation distribution between rainfall and EEPSSST for QBO and TO modes, respectively. For the QBO mode (Fig. 7), the correlation with phase of -3 and +6 months is significant. For -3-month phase-lag, there are negative centers over North China and over the south of the Changjiang River, and the central value over North China is below -0.45. That is to say the QBO peak of rainfall is ahead of that of EEPSSST by months. Three months later, these two centers still exist but with decreasing values. When the phase lag is +6 months, the original negative center over the middle and lower reaches of Changjiang River and south of it have become strongly positive with a value above 0.60. In addition, there are two positive centers respectively over Henan and the connecting area of Northeast China and North China. It is the positive center over Henan that propagates into Shaanxi-Gansu-Ningxia by the time of +9 months with a value above +0.45. Meanwhile, the center over the middle and lower reaches of the Changjiang River and south of it has decreased.

For TO mode, at phase lag of -5 months, North China, Southwest China, and Northwest China are regions with negative values, but East China with positive values. There is a center with a value below -0.60 over Shaanxi, Shandong and Sichuan. When the phase lag is 0 month, the value of the positive center over the middle and lower reaches of Changjiang River is higher than 0.60. After that, the center develops further and extends eastward. By the time of +15 months, the center has extended to Southwest China with a new center of 0.4; meanwhile a center of +0.50 emerges over Shanxi, Shaanxi and Inner Mongolia.

The above discussion indicates that although the correlation of the observational anomalies between rainfall and EEPSSST is insignificant, those for QBO and TO modes are significant. This is because the modes have different patterns and phases and they might cancel each other. Consequently, it is suggested that interannual oscillation components can reflect the effect of air-sea interaction more clearly than the time series itself.

## VI. CONCLUSION AND DISCUSSION

Some results can be summarized as follows:

- (1) Interannual variation of China's rainfall has significant components of QBO and TO;
- (2) Both QBO and TO modes of rainfall are pronounced over the middle and lower reaches of the Changjiang River and south of it, Shanxi, Shaanxi, eastern Gansu and central Inner Mongolia;
- (3) The modes have two different propagation ways, one originates from Northeast China and extends southwestward through North China to the eastern part of Northwest China and the northern part of Southwest China, while the other from Guangdong-Fujian area and propagates northward to the area between Huanghe and Huaihe Rivers and westward to Southwest China. Thus, they meet each other over North China. Therefore, it is speculated that the interannual oscillations of China's rainfall may come from the eastern Siberia and the Sea of Okhotsk, and from the tropical region such as the South China Sea and the Pacific Ocean;
- (4) The correlation between China's rainfall and EEPSSST is not significant, however,

the correlation between the interannual modes of these two elements is significant. This reflects the correlation between modes because of their different distributions and different phases. Thus, to investigate the effect of the air-sea interaction on the rainfall over China, it might be more useful to consider the signal of interannual oscillation;

(5) For both QBO and TO modes, the variation of EEPSSST is in phase with that of EISST and is out of phase with that of EWPSST. Thus, our research focuses not only on the variation of EEPSSST, but also on the variation of SST over the South China Sea and the equatorial western Pacific.

#### REFERENCES

- Bhalme, H.N. and Jadhav, S. K. (1984), The Southern Oscillation and its relation to the monsoon rainfall, *J. Climate*, **4**: 509–520.
- Chen Longxun, Yan Jinhua and Wang Gu (1989), The evolving features of interannual low-frequency oscillation and their relation to the occurrence of El Niño, *Acta Meteor. Sinica*, **3**:354–367.
- Huang Jiayou (1988), The manifestation of quasi-biennial oscillation in the monthly rainfall over China, *Scientia Atmos. Sci.*, **12**: 267–273 (in Chinese).
- Murakami, M. (1979), Large-scale aspects of deep convective activity over the Gate area, *Mon. Wea. Rev.*, **107**: 994–1013.
- Krishnamurti, T.N., Chub, S.H. and Iglesia, W. (1986), On the sea level pressure of the Southern Oscillation, *Arch. Met. Glop. Boil. (Ser. A.)* 385–425.
- Rasmusson, E.M., Ark in P.A. and Chen. W.Y. (1981), Biennial variation in surface temperature over the United States as revealed by singular decomposition, *Mon. Wea. Rev.*, **109**: 587–593.
- Reed, R.J., Campell, W.J., Rasmusson, E.M. and Roger, D.G. (1961), Evidence of a downward propagating annual wind reversal in the equatorial stratosphere, *J. Geophys. Res.*, **66**:813–818.
- Trenberth, K.S. and Shin, W.T.K. (1984), Quasi-biennial fluctuations in sea level pressures over the Northern Hemisphere, *Mon. Wea. Rev.*, **112**:761–777.
- Yan Jinhua, Chen Longxun and Wang Gu (1988), The propagating characteristics of interannual low-frequency oscillation in the tropical air-sea system, *Adv. Atmos. Sci.*, **5**:405–420.
- Yasunari, T. (1985), Zonally propagating modes of global east-west circulation associated with the Southern Oscillation, *J. Meteor. Soc. Japan*, **66**:1010–1026.
- Yasunari, T (1987), Global structure of the El Niño/Southern Oscillation, Part I: El Niño composites, Part II: The time evolution, *J. Meteor. Soc. Japan*, **65**: 67–80, 81–102.